Eur. Phys. J. B **21**, 191–204 (2001)

THE EUROPEAN PHYSICAL JOURNAL B

EDP Sciences

Exact diagonalization of the S = 1/2 XY ferromagnet on finite bcc lattices to estimate T = 0 properties on the infinite lattice

J. Schulenburg[1], J.S. Flynn[2,a], D.D. Betts[2], and J. Richter[1]

[1] Institute für Theoretische Physik, Universität Magdeburg, PO Box 4120, 39016 Magdeburg, Germany
[2] Department of Physics, Dalhousie University, Halifax, NS, B3H 3J5, Canada

Received 1st August 2000 and Received in final form 22 December 2000

Abstract. In this paper finite bcc lattices are defined by a triple of vectors in two different ways – upper triangular lattice form and compact form. In Appendix A are lists of some 260 distinct and useful bcc lattices of 9 to 32 vertices. The energy and magnetization of the $S = 1/2$ XY ferromagnet have been computed on these bcc lattices in the lowest states for $S_z = 0$, 1/2, 1 and 3/2. These data are studied statistically to fit the first three terms of the appropriate finite lattice scaling equations. Our estimates of the $T = 0$ energy and magnetization agree very well with spin wave and series expansion estimates.

PACS. 05.50.+q Lattice theory and statistics (Ising, Potts, etc.) – 75.10.Jm Quantized spin models – 75.50.Dd Nonmetallic ferromagnetic materials

1 Introduction

The physics of quantum spin systems on lattices of $d = 1$, 2 and 3 dimensions has been much studied for several decades. Several different models have been studied including the Heisenberg antiferromagnet, the t-J model, the Hubbard model, the spin fermion model, the spin-orbital model and the XY ferromagnet. There are several different methods to study quantum spin models, especially in one dimension. While experiments never reach $T = 0$, several do work at extremely low temperature. In three dimensions, as opposed to two dimensions, the zero temperature properties are very similar to those at very low temperature.

Useful methods to study quantum spin models such as the $S = 1/2$ Heisenberg and XY models at $T = 0$ in three dimensions ($d = 3$) include series expansion, [1,2], spin wave, [3–5], and variational [6] methods (many other references could be cited). The $S = 1/2$ Heisenberg antiferromagnet is generally regarded as the most important quantum spin model on a lattice, and studies of this model in one, two and three dimensions are very numerous. However, the spin one-half XY model is also quite important as it is the simplest fully quantum mechanical lattice model. Recent (1999) examples have used quantum Monte Carlo and/or finite lattice method on the square lattice [7–9]. In this $d = 3$, $T = 0$ regime we use the latest method – exact diagonalization of quantum spin models on finite three-dimensional lattices [10–12].

[a] e-mail: flynnjs@is2.dal.ca

Each finite lattice in three dimensions can be derived from one or more parallelepipeds. Such a parallelepiped can be defined by three edge vectors in such a length and direction as to have a lattice vertex on each of the eight parallelepiped corners. Thus a set of identical, regularly packed parallelepipeds will completely fill the infinite lattice – a "three-dimensional tiling". A $d = 3$ lattice is formed by identifying each pair of opposite faces of the parallelepiped as being one and the same face. More detail is described in Section 2 below. In particular, the very useful *upper triangular lattice form* is described in Section 2.

Section 3 describes the generation of finite bcc lattices that can be used for *ferromagnetic* models. The number of such bcc lattices of $N \leq 32$ vertices is an order of magnitude greater than the number of *bipartite* lattices needed for the study of an antiferromagnetic model. This section also explains the *geometric imperfection*, $I_{\rm G}$, of finite lattices. If $I_{\rm G}/N$ for a specific finite lattice is too large, that finite lattice is not used. An $N = 15$ example of a bcc lattice is shown in Figure 1. The description of all the useful bcc lattices used is listed in Appendix A. Each distinct lattice is labelled $N.i$.

Section 4 describes the computation of physical properties of the $S = 1/2$ XY ferromagnet on finite bcc lattices in the ground state and in the first excited state. Specifically we needed about seventy hours to calculate the eigenstate of the largest Hamiltonian ($N = 32$) using an SGI Power-Challenge with 2GB of memory. The detailed results are shown in Appendix B.

In Section 5 statistical analysis estimates the $T = 0$ properties of the $S = 1/2$ XY ferromagnet on the infinite body-centred cubic lattice. The data for physical properties of this model on finite bcc lattices are statistically analysed in order to obtain the estimates of the first two or three coefficients of the appropriate finite lattice scaling equation. The results are displayed in Tables 2, 3, 4 and 5.

Summary, conclusions and outlook are described in Section 6.

2 Definition of finite bcc lattices

This process has been described in an earlier paper [12] but some aspects, new or repeated, will be displayed here. The infinite bcc lattice can be defined by any three of the four primitive vectors:

$$\mathbf{a}_1 = (1,1,1), \quad \mathbf{a}_2 = (1,1,-1),$$
$$\mathbf{a}_3 = (1,-1,1) \quad \text{and} \quad \mathbf{a}_4 = (-1,1,1). \tag{1}$$

The infinite bcc lattice can be "filled" (the three-dimensional analogy of "tiled" in two dimensions) by any one of several sets of an ascending number of identical parallelepipeds. Such a parallelepiped is defined by three edge vectors,

$$\mathbf{L}_\alpha = \sum_{\beta=1}^{3} n_{\alpha\beta}\mathbf{a}_\beta, \tag{2}$$

in which each $n_{\alpha\beta}$ is an integer. Each of three integers $n_{\alpha1}$, $n_{\alpha2}$ and $n_{\alpha3}$ are odd or each are even. A finite bcc lattice can be derived from any bcc parallelepiped defined by (2) by applying a full set of three periodic boundary conditions. That is, each pair of the opposite faces of the parallelepiped are defined to be identical. In other words, each finite lattice is the three-dimensional analogue of a two-dimensional torus.

Figure 1 provides a concrete example, a parallelepiped that is turned into a finite bcc lattice with fifteen distinct vertices. The original parallelepiped's eight corners are labeled C_1, C_2, ..., C_8. The four vertices on four of the twelve edges of the parallelepiped are labeled E_1, E_2, E_3 and E_4, and the two vertices on one pair of opposite faces of the parallelepiped are labeled F_1 and F_2. This parallelepiped contains also twelve *internal* vertices we could label as A, B, D, G, H, I, J, K, L, M, N and P. However, it appears simpler not to show these internal vertices in Figure 1. The three defining edge vectors from C_8 to C_1, C_2 and C_3 respectively are $\mathbf{L}_1 = (1,-1,3)$, $\mathbf{L}_2 = (-1,3,3)$ and $\mathbf{L}_3 = (4,2,0)$. The volume of this parallelepiped, $V = \mathbf{L}_3 \cdot (\mathbf{L}_2 \times \mathbf{L}_1) = 60$.

By identifying the three pairs of opposite faces of this parallelepiped, *i.e.* applying periodic boundary conditions, the two face vertices F_1 and F_2 become F, the four edge vertices, E_1, E_2, E_3 and E_4 become one other vertex E, and the eight corner vertices C_1, C_2, ..., C_8 are all now the single vertex C. The finite bcc lattice thus formed contains fifteen vertices A, B, C, D, E, ..., P. A finite lattice has

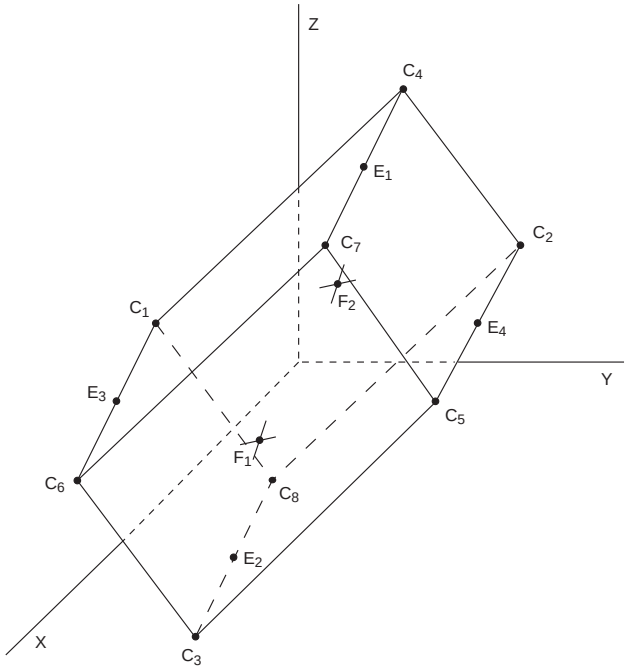

Fig. 1. A parallelepiped of $N = 15$ vertices embedded in an infinite bcc lattice. By identifying each pair of opposite faces this parallelepiped becomes a finite bcc lattice of fifteen vertices.

no faces, edges nor corners, and all vertices have the same geometric environment.

In fact, a typical finite lattice can be derived from any one of several parallelepipeds and thus it might appear to be several distinct finite lattices. However, it has been proved by Lyness *et al.* [13] that, in effect, each parallelepiped in any number of dimensions, d, defined by a matrix in upper triangular lattice form (utlf) will, upon complete application of periodic boundary conditions, form a unique finite lattice.

A d-dimensional utlf matrix, L^{t}, must satisfy the following criteria:

$$\begin{aligned} &\mathrm{L}^{\mathrm{t}}_{ii} \geq 1 && i = 1,2,\ldots,d \\ &\mathrm{L}^{\mathrm{t}}_{ij} = 0 && 1 \leq j < i \leq d \\ &\mathrm{L}^{\mathrm{t}}_{ij} \in [0, \mathrm{L}^{\mathrm{t}}_{jj}) && 1 \leq i < j \leq d \\ &\mathrm{L}^{\mathrm{t}}_{i+1,i+1} \geq \mathrm{L}^{\mathrm{t}}_{ii}. \end{aligned} \tag{3}$$

In particular, in an unbounded three-dimensional lattice, the defining utlf matrix is

$$\mathrm{L}^{\mathrm{t}} = \begin{pmatrix} \mathbf{L}^{\mathrm{t}}_1 \\ \mathbf{L}^{\mathrm{t}}_2 \\ \mathbf{L}^{\mathrm{t}}_3 \end{pmatrix} \tag{4}$$

where the $\mathbf{L}^{\mathrm{t}}_i$ are the defining vectors.

Furthermore, on the infinite bcc lattice defined by the above primitive defining vectors $\mathbf{a}_\beta$, the number of

vertices, N, in a finite utlf description of a finite bcc lattice requires

$$\mathrm{L}_{11}^{\mathrm{t}}\mathrm{L}_{22}^{\mathrm{t}}\mathrm{L}_{33}^{\mathrm{t}} = 4N. \tag{5}$$

Since $\mathbf{L}_3^{\mathrm{t}}$ lies on the Z-axis and $\mathbf{L}_2^{\mathrm{t}}$ lies in the YZ-plane all of their components are even integers. In particular, the utlf vectors defining the $N = 15$ finite bcc lattice 15.28, described above, are $\mathbf{L}_1^{\mathrm{t}} = (1, 1, 9)$, $\mathbf{L}_2^{\mathrm{t}} = (0, 2, 6)$ and $\mathbf{L}_3^{\mathrm{t}} = (0, 0, 30)$.

There is a second way of describing a finite lattice. Have a parallelepiped defined by three *compact edge vectors*, $\mathbf{L}_i^{\mathrm{c}}$, such that not one of the six distinct face diagonals joining a pair of corner vertices will have a length less than any of the compact edge vectors. These compact vectors are easily obtained by linear matrix multiplying the utlf matrix. The edge vectors, $\mathbf{L}_1^{\mathrm{c}}$, $\mathbf{L}_2^{\mathrm{c}}$ and $\mathbf{L}_3^{\mathrm{c}}$, of the above example of $N = 15$ vertices of the parallelepiped are the set of compact defining vectors for this finite bcc lattice.

3 Generation of finite ferromagnetic bcc lattices

From equations (1) and (2) it is clear that, in each of the three vectors defining a finite bcc lattice, each of its components are odd or each are even. For a *bipartite* finite bcc lattice, all components of each of the defining vectors are even. In a recent paper [12] on the $S = 1/2$ Heisenberg antiferromagnet using exact diagonalization on bipartite lattices only (of course), we found a total of forty useful bipartite bcc lattices with $16 \leq N \leq 32$ vertices. The defining vectors are listed in Table 2 of that paper. The smallest bcc bipartite lattice of use has $N = 16$ vertices so that each vertex would have a complete set of nearest neighbours on the other sublattice. The large diagonalization time on the computer meant that bipartite lattices of $N > 32$ would not be useful.

In this paper on the $S = 1/2$ XY ferromagnet exact diagonalization can be used on all finite bcc lattices. Furthermore we felt that finite lattices of as few as $N = 9$ vertices would sometimes be suitable as each vertex would have a complete set of eight neighbours. Nevertheless more often finite bcc lattices need to have $N \geq 15$ so that each vertex would have a complete set of second neighbours also.

Here we show in Table 1 that for $9 \leq N \leq 25$ there is a total of 72 odd-N bcc lattices, for $10 \leq N \leq 26$ there is a total of 125 even-N bcc lattices. Only 13 of these 125 bcc lattices are bipartite and therefore usable for exact diagonalization of Hamiltonians of antiferromagnetic models. However, for $16 \leq N \leq 32$ there are 40 bipartite bcc lattices – enough to use in the statistical estimates of the properties of the $S = 1/2$ Heisenberg antiferromagnet at $T = 0$.

In Table 1 we also show that for $9 \leq N \leq 32$ there are 156 odd-N bcc lattices and 306 even-N bcc lattices, of which 181 have $N = 28$, 30 or 32 vertices. For computation time purpose we decided not to include so many more even-N bcc lattices. In the last double column, the numbers of the finite bcc lattices most useful for the exact diagonalization method are listed.

Table 1. Numbers of distinct finite odd/even bcc lattices and useful distinct lattices of $9 \leq N \leq 32$ vertices. n is the total number of lattices, n_{b} is the number of bipartite lattices and ν is the number of useful lattices for each value of N.

N	n	n_{b}	ν
9/10	1/1	0	1/1
11/12	1/2	0	1/2
13/14	2/3	0	2/3
15/16	7/6	1	7/6
17/18	5/13	1	4/12
19/20	7/18	2	6/16
21/22	17/15	1	16/13
23/24	12/42	6	11/36
25/26	20/25	2	14/19
Subtotals	72/125	13	62/108
27/28	36/45	5	25/32
29/30	22/67	7	16/44
31/32	26/69	15	17/50
Totals	156/306	40	120/234

The geometric criterion we used to get rid of a minority of poor lattices is that the geometric imperfection, I_{G}, of each lattice divided by N should be less than 0.35. Geometric imperfection, for finite simple cubic lattices, was first introduced by Betts and Stewart [10]. In an *infinite* bcc lattice each vertex has geometrically $N_1 = 8$ nearest neighbours, $N_2 = 6$ second nearest neighbours, $N_3 = 12$ third, $N_4 = 24$ fourth, $N_5 = 8$ fifth, ... N_k of kth neighbours. We can call these "shells" of neighbours about any vertex. In a *finite* lattice with an *odd* number, N, of vertices one vertex, labelled A, is chosen arbitrarily and temporarily as a centre or origin. Then the remaining $N - 1$ vertices are automatically paired, say B & C, D & E, ... in such a way that, under inversion in A, the other vertices interchange B $\leftrightarrow$ C, D $\leftrightarrow$ E, etc.

Now consider a *finite* lattice of N vertices in which all shells below the k shell are full. If the k shell is not full it will have $N_k - 2$, $N_k - 4$ or ... 0 vertices. But if all shells above it are empty the finite lattice has geometric perfection; $I_{\mathrm{G}} = 0$. However, if the $k+1$ shell above it has a pair of vertices and all shells above that are empty, then $I_{\mathrm{G}} = 2$.

The geometric imperfection of 4 can occur in two ways: (a) if shell $k - 1$ has $N_{k-1} - 2$ vertices, the shell k has N_k vertices and the shell $k + 1$ has 2 vertices then $I_{\mathrm{G}} = 4$, or (b) if shell k has $N_k - 4$ vertices and the last occupied shell, $k + 1$, has 4 vertices, $I_{\mathrm{G}} = 4$.

Let us again use the example of $N = 15$ lattice 15.28. Any vertex of this lattice has 8 nearest neighbours, only 4 second nearest neighbours and 2 third nearest neighbours. Thus the geometric imperfection $I_{\mathrm{G}}(15.28) = 2$. Another $N = 15$ lattice, 15.577, has 8 nearest neighbours and 6

second nearest neighbours of any vertex. So this lattice is a perfect $N = 15$ bcc lattice with $I_{\rm G}(15.577) = 0$.

Determining the geometric imperfection of an even N lattice is just a bit different. Again one vertex is chosen as the temporary origin and $N - 2$ vertices are thus paired so that under inversion in the origin, A, the pairs of other vertices exchange B $\leftrightarrow$ C, D $\leftrightarrow$ E, ... However, the remaining vertex, Z, stays where it is under inversion in A. Thus A and Z are temporarily the poles. Because pole Z may be farther from the origin than in a perfect finite lattice, it means that geometric imperfections in even N lattices can be odd or even. The simplest example among finite bcc lattices is an $N = 12$ vertex lattice labeled 12.17. It has defining vectors in compact form $\mathbf{L}_1^{\rm c} = (1, -1, 3)$, $\mathbf{L}_2^{\rm c} = (-1, 3, 1)$ and $\mathbf{L}_3^{\rm c} = (4, 2, 0)$. There is a complete set of four pairs of nearest neighbours, one pair of second nearest neighbours and a single third neighbour, so $I_{\rm G}(12.17) = 1$. On the other hand, the twelve vertex bcc lattice 12.25 has four pairs of nearest neighbours, one pair of second neighbours and a single second neighbour to any vertex. Thus $I_{\rm G}(12.25) = 0$.

We have a computer program that can obtain, in utlf form, all finite lattices of any number of vertices, N, on any infinite bipartite lattice in two or three dimensions. The program can also yield for each finite lattice the geometrical imperfection, $I_{\rm G}$, the topological imperfection, $I_{\rm T}$, the rotational symmetry in Schoenfliess notation, S, and whether or not the finite lattice is bipartite. (The topological imperfection is not used in this article, but it was described in our previous paper [12].) If we were studying a Heisenberg antiferromagnet only bipartite finite lattices could be used. However, as we have been studying an $S = 1/2$ XY *ferromagnet* on the infinite bcc lattice we could and did use both bipartite and nonbipartite finite bcc lattices of even N and also finite bcc lattices of odd N vertices.

After considerable computing and statistical analysis we decided that only those finite bcc lattices with $I_{\rm G}/N < 0.35$ should be used. The finite bcc lattices must have at least $N = 9$ vertices, otherwise no vertex would have a complete set of eight nearest neighbours. We stopped at bcc lattices of $N = 32$ because diagonalization of Hamiltonians on lattices with more than 32 vertices would require an excessive amount of computer memory and especially time. The finite bcc lattices now suitable are described in Tables A.1, A.2 and A.3. Notice that there are 116 ferromagnetically useful odd-N bcc lattices of $15 \leq N \leq 31$ and 102 even-N bcc lattices of $16 \leq N \leq 26$. For $N = 28$, 30 and 32 there are 27 bipartite bcc lattices, because we decided 245 finite bcc lattices would be sufficient. After all, in the earlier paper [12] a total of 40 bipartite lattices of $16 \leq N \leq 32$ seemed sufficient. There are another 99 nonbipartite bcc lattices of $N = 28$, 30 and 32.

4 Computation of physical properties of the S = 1/2 XY ferromagnet on finite bcc lattices

The Hamiltonian of the spin one-half XY ferromagnet in zero magnetic field is

$$H = J \sum_{\langle i,j \rangle} (S_i^x S_j^x + S_i^y S_j^y) \tag{6}$$

where the sum is over nearest neighbour pairs of vertices. It was proved by Lieb and Mattis [14] that the ground state of this model on an infinite three-dimensional lattice has total spin component in the z-direction equal to zero and is nondegenerate. The first excited state has the z component of the total spin equal to one or minus one. Later it was proved by Kennedy *et al.* [15] and Kubo and Kishi [16] that this model has long range order, $m_\perp^2 = \langle m_x^2 + m_y^2 \rangle = 2\langle m_x^2 \rangle$, in the ground state (and obviously for $T < T_{\rm c}$).

All of the finite bcc lattices are translationally invariant and invariant under inversion, so this simplifies the diagonalization of the Hamiltonians. On the even-N bcc lattices the ground state Hamiltonian submatrix has the z component of the total spin $S_z = 0$. The first excited state submatrix has $S_z = \pm 1$. On the odd-N bcc lattices the ground state has the z component of the total spin $S_z = \pm 1/2$. The first excited state has $S_z = \pm 3/2$. In the Hamiltonian diagonalizations we use the submatrices with positive S_z's.

On each of the submatrices of the Hamiltonian the ground state energy and its corresponding eigenvectors have been calculated. The Lanczos technique used in the diagonalization is standard [17]. On the even-N bcc lattices we computed on the $S_z = 0$ submatrix the ground state energy $E_0 = N\epsilon_0$ and on the $S_z = 1$ submatrix the first excited state energy, $E_1 = N\epsilon_1$. Using the ground state and first excited state eigenvectors we computed the square of the magnetizations in the spin-space X-direction, $\langle m_x^2 \rangle$. Hence we immediately obtained on each even-N bcc lattice $m_{x,0}$ and $m_{x,1}$ respectively. The computations have been made on all even-N lattices of $10 \leq N \leq 26$ vertices, and on bipartite lattices only for $28 \leq N \leq 32$. On all odd-N bcc lattices of $9 \leq N \leq 31$ we computed on the $S_z = 1/2$ Hamiltonian submatrix the ground state energy $E_{1/2} = N\epsilon_{1/2}$ and on the $S_z = 3/2$ submatrix the first excited state energy $E_{3/2} = N\epsilon_{3/2}$.

If any two geometrically distinct finite bcc lattices have the same ground state and first excited state energies then they are topologically identical, and only one of them would be used. The computed results are listed in Tables B.1 and B.2 for all finite bcc lattices used.

In Table B.1 we show the dimensionless energies per vertex, ϵ_s, for the $S_z = 1/2$ ground state, the lowest excited $S_z = 3/2$ state energy and the ground state magnetization squared on all odd-N bcc lattices of $9 \leq N \leq 31$, for which $I_{\rm G}/N < 0.35$. The total number of such bcc lattices is 120; of these odd-N lattices 33 have more than 28 vertices.

In Table B.2 we also show ϵ_s for the $S_z = 0$ ground state, the lowest $S_z = 1$ state energy and the ground state magnetization squared on all even-N bcc lattices of $10 \leq N \leq 26$ and for which $I_{\rm G}/N < 0.35$. There is a total of 108 such lattices. Among these lattices only 13 are bipartite and hence suitable for exact diagonalization of the Hamiltonians of *antiferromagnets* such as the $S = 1/2$ Heisenberg antiferromagnet [12].

Of even-N bipartite lattices with $N = 28$, 30 or 32 for which $I_{\rm G}/N < 0.35$ there are only 27. However, there are 99 nonbipartite bcc lattices of $28 \leq N \leq 32$. It would thus have taken, for these lattices, several thousands of hours of computer time to diagonalize all the $S_z = 0$ and $S_z = 1$ submatrix Hamiltonians of the $S = 1/2$ XY ferromagnet. Thus we use only the bipartite bcc lattices in this range.

Statistical analysis of these data will be described in the next section. The purpose is to derive the $T = 0$ physical properties on the infinite bcc lattice.

5 Statistical analysis estimation of the T = 0 properties of the S = 1/2 XY ferromagnet on the infinite body-centred cubic lattice

In order to estimate any physical properties of the $S = 1/2$ XY ferromagnet on the infinite bcc lattice, using the exact diagonalization data for that property on the finite bcc lattices, one must fit the data statistically to the appropriate finite lattice scaling equation. The independent variable in such equations is L^{-1} defined by $L^3 = N$, the number of vertices. For example, the energy of the XY ferromagnet finite lattice scaling equation for any total spin S_z (or for simplicity below, s) is in three dimensions

$$\epsilon_s(L) = \epsilon_s(\infty) + A_4^s L^{-4} + A_6^s L^{-6} + ... \qquad (7)$$

Such scaling equations are explained carefully in the paper by Hasenfratz and Niedermayer [18], and earlier papers on this matter [19–21] are cited therein. Oitmaa *et al.* [2] used both series expansions and spin wave methods on the $S = 1/2$ Heisenberg antiferromagnet on the simple cubic and bcc lattices to obtain estimates of the first term and the second term of equation (7). They obtained estimates of the ground state energy per vertex, $\epsilon_0(\infty)$ from the first term and spin wave velocity, v, from the second term.

In the pioneering application of the method of exact diagonalization of the finite lattices of the $S = 1/2$ XY ferromagnet on simple cubic lattices [10] it was quickly noticed that the curve fitting the $\epsilon_{1/2}$ data from odd-N simple cubic lattices was definitely above the curve fitting the ϵ_0 data from even-N lattices. Moreover, here we also have data for ϵ_1 on even-N and $\epsilon_{3/2}$ on odd-N bcc lattices. It is clear that while on finite lattices $\epsilon_1 > \epsilon_0$ and $\epsilon_{3/2} > \epsilon_{1/2}$, on the *infinite* lattices one should expect $\epsilon_0 = \epsilon_{1/2} = \epsilon_1 = \epsilon_{3/2}$. Similarly, we should expect $A_4^0 = A_4^{1/2} = A_4^1 = A_4^{3/2}$ on the infinite lattices in three dimensions.

Clearly we do not study the energies, E_s, of the $S = 1/2$ XY ferromagnet (or other models) but the dimensionless energies per vertex, $\epsilon_s = E_s/NJ$. Nevertheless, on finite lattices ϵ_s depends on both the number of vertices, N, and the geometric arrangement of those N vertices on these finite bcc lattices so our energy density label is $\epsilon_s(N.i)$.

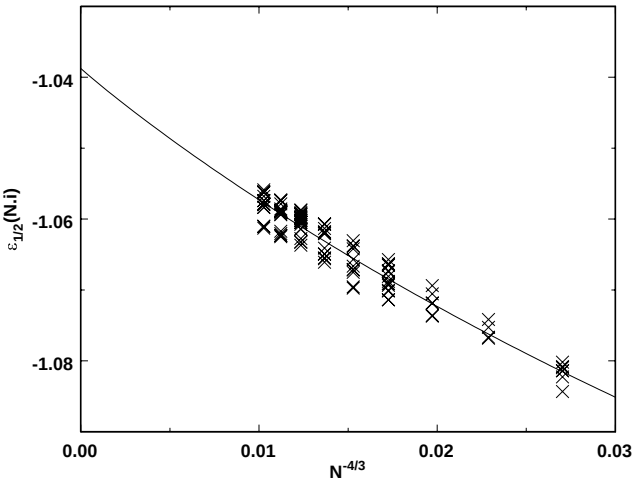

Fig. 2. Above each horizontal position at $N^{-4/3}$ for $N =$ 15, 17, 19, ..., 31 is a set of points representing the bcc XY ferromagnet energies per vertex, $\epsilon_{1/2}(N.i)$, of each of the finite bcc lattices of N vertices. The statistical curve fitted to these points is $\epsilon_{1/2}(N) = \epsilon(\infty) + A_4^{1/2} N^{-4/3} + A_6^{1/2} N^{-2}$.

Our statistical analyses have used sets of $\epsilon_s(N.i)$ data for $N \geq 15$, which means that in each finite bcc lattice each vertex can have a complete shell of nearest neighbours and a complete shell of second nearest neighbours. As an example of the scatter of the ground state energy per vertex, $\epsilon_{1/2}(N.i)$, of the $S = 1/2$ XY ferromagnet in each of nine sets of vertices $15 \leq N \leq 31$ is displayed in Figure 2. Notice that a small number of the points in each of the nine sets of clusters are "outriders" relatively far from the centre of the cluster and are not statistically useful. Statistical analysis of these data determines the numerical coefficients of equation (7) and hence the curve in Figure 2. We also exclude data from finite lattices for which the geometric imperfection, $I_{\rm G} \geq 0.35$. Clearly the smaller sets of data are better because the statistical estimates of $\epsilon_s(\infty)$ and of A_4^s are considerably closer to one another when $N \geq 15$ than they are when $N \geq 9$ data are used. Accordingly in Table 2 we display only the statistical estimates obtained using data of $N \geq 15$ and $I_{\rm G} < 0.35$.

In Table 2 we have displayed $\epsilon_s(\infty)$, A_4^s and A_6^s, the coefficients in equation (7) for $s = 0$, 1/2, 1 and 3/2. Indeed for $s = 0$ and $s = 1$ we have obtained separate statistical estimates using only bipartite lattices (B) and only nonbipartite lattices (Nb). (Of course, all finite bcc lattices of odd N must be nonbipartite.) Notice that to four digits $\epsilon_s^{\rm Nb}(\infty) = -1.039$ for each of the four Nb sets of $s = 0$, 1/2, 1 and 3/2. On the other hand $\epsilon_0^{\rm B}(\infty) = \epsilon_1^{\rm B}(\infty) = -1.042$. The averages are respectively $\epsilon^{\rm Nb}(\infty) = -1.0389$ and $\epsilon^{\rm B}(\infty) = -1.0417$. We must conclude that the $\epsilon^{\rm Nb}(\infty)$ average estimate, using some two hundred nonbipartite lattices, is more accurate than $\epsilon^{\rm B}(\infty)$ using only forty bipartite lattices.

Table 2. Statistically analysed coefficients of energy equation (7) using ground states or first excited states on even-N or odd-N bcc lattices. B means bipartite and Nb means nonbipartite.

Data sets	S_z	$\epsilon_s(\infty)$	A_4^s	A_6^s
$16 \le N \le 26$, Nb	0	−1.0393(1)	−2.22(3)	2.8
$16 \le N \le 32$, B	0	−1.0418(5)	−1.71(3)	1.3
$15 \le N \le 31$, Nb	1/2	−1.0388(1)	−2.27(4)	4.2
$16 \le N \le 26$, Nb	1	−1.0391(3)	−2.26(5)	7.5
$16 \le N \le 32$, B	1	−1.0417(2)	−1.75(5)	6.0
$15 \le N \le 31$, Nb	3/2	−1.0385(4)	−2.35(11)	13.4

As it is known [18], the second coefficient, A_4^s, of the finite lattice scaling equation is independent of s. In Table 2 the average of the four nonbipartite estimates is $A_4^{\rm Nb} = -2.27$, considerably larger than the average $A_4^{\rm B} = -1.73$. It is also known that A_6^s does increase substantially as s increases, and our Table 2 shows the accelerating increase of A_6^s from $s = 0$ to $s = 3/2$.

According to Oitmaa *et al.* [2] and others [18–20], on the bcc lattice $-A_4 = \beta v/2$ where the geometric shape factor $\beta = 2.1104607$ and v is the spin wave velocity. Using the average estimate of A_4 we obtain $v = 2.15(2)$. (Oitmaa *et al.* [2] give β for the bcc lattice as different by a factor of $2^{4/3}$ from what we show here. This is due to the fact that they use $L^3 = N/2$ where we use $L^3 = N$.)

Because we have used approximately two hundred and sixty finite lattices of $15 \le N \le 32$ vertices, we would fully clutter any figure with so many points. However, we can insert a much smaller set of points (together with curves) in our figures and thus avoid clutter. For each N there is a subset of exact diagonalization values; the averages only of these physical properties provide points in the appropriate figure. Such a figure will also contain one or more curves representing the finite lattice scaling equation determined statistically by using *all* useful data not just the averages at each N.

Figure 3 is an example with four curves representing scaling equation (7), $S_z \equiv s = 0$, 1/2, 1 and 3/2, and about 40 averaged points, $\epsilon_s(N) = \langle \epsilon_s(N.i) \rangle$. Which points with which S_z is shown in the upper right Figure 3. For even N we have used only the data for nonbipartite lattices.

All the curves in Figure 3 reach the same point, $\epsilon(\infty)$, on the vertical axis. Furthermore, each of the four curves has the same slope, A_4 at $1/L^4 = 0$. However, the curvature increases rapidly with S_z. These effects demonstrate the data in Table 2.

For each of three reasons it is certain that A_6^s is not independent of s. First, from Table 2 it is clear that $A_6^0 < A_6^{1/2} < A_6^1 < A_6^{3/2}$. Second, the finite lattice scaling equation curves in Figure 3 have a greater curvature the larger S_z is. Finally, Hasenfratz and Niedermayer [18] show that

$$[\epsilon_1(L) - \epsilon_0(L)] = D_6 L^{-6} + D_8 L^{-8} + ... \qquad (8)$$

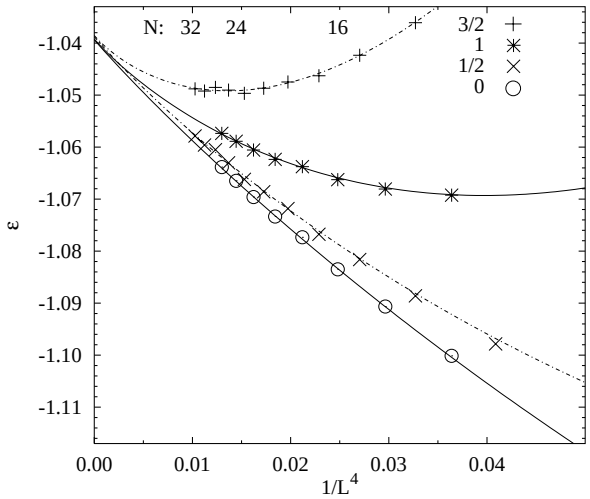

Fig. 3. Energy per vertex, ϵ, against L^{-4} for $S_z = 3/2$, 1, 1/2 and 0. The points are the averages, $\epsilon_s(N)$, for each set of S_z and N. The curves are from equation (7).

Table 3. Statistically analysed coefficients of bcc finite lattice data of equation (9) where D_n are coefficients of even N data and D'_n are equations for odd N.

Coefficients and	Number of terms in the scaling equation		
their ratios	one term	two terms	three terms
D_6	4.4119	4.2531	4.2800
D'_6	8.7844	8.5087	8.5654
D'_6/D_6	1.9911	2.0006	2.0013
D_8	—	1.022	0.624
D'_8	—	1.995	1.150
D'_8/D_8	—	1.95	1.84

In three dimensions this means that $\epsilon_1(\infty) - \epsilon_0(\infty) = 0$ and that $A_4^1 - A_4^0 = 0$ but $A_6^1 - A_6^0 = D_6 \neq 0$. Further, $D_6 = 1/2\chi_\perp$, the inverse susceptibility. We define $\Delta = \epsilon_1(L) - \epsilon_0(L)$ and $\Delta' = \epsilon_{3/2} - \epsilon_{1/2}$. Then our statistical analysis of even-N bcc $S = 1/2$ XY ferromagnet data obeys the scaling equation

$$L^6 \Delta = D_6 + D_8 L^{-2} + ... \qquad (9)$$

with the same form for odd-N.

This shows that $D_0 = D_1 = ... D_5 = D_7 = 0$. These data also show that D_6 and D_8 are not equal to zero. After observing graphs and examining Table 3 we believe that the two-term scaling equations are best.

Based on the average of the three of our ratios in Table 3, $D'_6/D_6 = 1.998(1)$, clearly $D'_6 = 2D_6$. The averages in the two ratios $D'_8/D_8 = 1.90(2)$ indicate also that $D'_8 \sim 2D_8$. These factors of 2 arise from equation (2.19) in the paper of Hasenfratz and Neidermayer [18].

The susceptibility, $\chi_\perp$, is defined as $\chi_\perp = 1/2D_6 = 1/D'_6$ according to Hasenfratz and Neidermayer [18]. Using

Table 4. Statistical results of fitting equation (11) to the finite lattice data for $m_{\perp,s}$. The Odd-N and Even-N, bipartite data were taken in the range from $15 \leq N \leq 32$. The Even-N, nonbipartite data were in the range $16 \leq N \leq 26$.

Data set of lattices	S_z	$m_\perp(\infty)$	B_2	B_4
Odd-N	1/2	0.478(1)	0.31(2)	−0.03
Even-N, bipartite	0	0.478(1)	0.27(3)	0.2
Even-N, nonbipartite	0	0.485(1)	0.19(3)	0.5

Table 3 these coefficients in the column of two terms the estimates of $\chi_\perp$ are 0.1176 and 0.1175 so we take the average $\chi_\perp = 0.1176(4)$. Without calculating the spin stiffness, ρ_s, directly, but using the data above, $\rho_s = v^2\chi_\perp = 0.55(4)$.

Now we turn to the magnetization. Oitmaa *et al.* [2], following Neuberger and Ziman [20], determined by effective Lagrangian theory that the second term in the finite lattice scaling equation for the staggered magnetization is proportional to L^{d-1}. Thus for the Heisenberg *antiferromagnet* in three dimensions the finite lattice scaling equation for the *staggered magnetization* is

$$m^+(L) = m^+(\infty) + B_2 L^{-2} + ... \tag{10}$$

In our paper [12] on the $S = 1/2$ Heisenberg antiferromagnet on the bcc lattices we found *via* our statistical analyses that

$$m^+(L) = m^+(\infty) + B_2 L^{-2} + B_4 L^{-4} + ... \tag{11}$$

The XY ferromagnet on bipartite lattices has a magnetization, $m_\perp(L)$, that is identical to the XY antiferromagnet's m^+. Thus we expect the same finite lattice scaling equation for $m_\perp(L)$ on the set of all bcc lattices. The data that we list in Appendix B is the magnetization squared in the X spin space direction. We decided later that it was more convenient to deal with $m_\perp$ so the data were converted according to $m_\perp = \sqrt{2m_x^2}$.

Our statistical analyses of the magnetization of the $S = 1/2$ XY ferromagnet on bcc lattices found that the finite lattice scaling equation for the magnetization, $m_\perp$, is indeed of the same form as (11). (Our guess is that a fourth term might well be B_6/L^6.)

Table 4 shows that the estimates of $m_\perp(\infty)$ and B_2 using the bipartite even-N lattices are closer to the estimates of the same properties using the odd-N lattices than those using the nonbipartite even-N lattices. This may be due to the fact that the latter data stop at $N = 26$ while the first two go to 31 and 32 respectively.

Equation (52) in Oitmaa *et al.* [2] implies that

$$B_2 = \Sigma v\gamma/\rho_s \tag{12}$$

for the Heisenberg antiferromagnet in three dimensions. Σ is their $m^+(\infty)$ and γ is another shape factor. As $m_\perp$ scales the same as m^+, there is no reason why (12) shouldn't apply for $m_\perp$ and we obtain a means to check our earlier result for ρ_s. In our notation, (12) becomes

$$\rho_s = m_\perp(\infty)v\gamma/B_2 \tag{13}$$

where $m_\perp(\infty) = 0.480$, $B_2 = 0.29$ (averaging from the top two estimates of Tab. 4), $\gamma = 0.1792055$ (from [2]) and $v = 2.16$, our earlier result (again, our value of γ is a factor of $2^{2/3}$ different from that given in [2], for the same reason as stated before concerning β). This gives us a second estimate of $\rho_s = 0.64$. This agrees quite well with our earlier estimate of $\rho_s = 0.55$ given the indirect route of each estimate.

After statistically analysing the magnetization data to estimate the coefficients $m_\perp(\infty)$, B_2 and B_4 in finite lattice scaling equation (11) the question arises as to whether some of these coefficients, like the coefficients $\epsilon(\infty)$ and A_4 in (7), are independent of the spin state of the data. Compared with the energy per vertex, there is not the same physical importance to study $m_\perp$ finite lattice data above the ground states, $S_z = 0$ for even-N and $S_z = 1/2$ for odd-N lattices. Nevertheless, after studying the $L^6(\epsilon_s - \epsilon_{s-1})$ finite lattice data we decided to study $L^n(m_{\perp,0} - m_{\perp,1})$ data. For $m_{\perp,1}$ we had data only for bipartite bcc lattices of $16 \leq N \leq 26$. We soon found that $n = 6$ was the appropriate exponent of L above, and that in the finite lattice scaling equation (11) $m_{\perp,1}(\infty) = m_{\perp,0}(\infty)$, $B_2^1 = B_2^0$ and $B_4^1 = B_4^0$, as well as our small amount of data showed. We then used a scaling equation analogous to (9), namely

$$L^6\Gamma \equiv (m_{\perp,0} - m_{\perp,1})L^6 = F_6 + F_8 L^{-2} + ... \tag{14}$$

We found that with two terms in (14)

$$L^6\Gamma = 0.942 - 0.17L^{-2}. \tag{15}$$

If it were of greater physical interest we could readily compute many $m_{\perp,3/2}$ data and more $m_{\perp,1}$ data especially on nonbipartite even-N finite bcc lattices.

6 Summary, conclusions and outlook

Following our earlier paper [12] on the $S = 1/2$ *Heisenberg antiferromagnet* on finite even-N *bipartite* lattices, we have here extended the generation of finite bcc lattices to include all *nonbipartite* lattices, of $9 \leq N \leq 31$ odd lattices and of $10 \leq N \leq 32$ even lattices. We have found it useful statistically to delete the small fraction of these lattices for which the geometric imperfection, I_G, is greater than or equal to 0.35 N and to delete also lattices of fewer than $N = 15$ vertices.

On each of the remaining even-N bcc lattices of $10 \leq N \leq 26$ we computed, in the lowest state of $S_z = 0$ and of $S_z = 1$, of the $S = 1/2\,XY$ ferromagnet Hamiltonian the dimensionless energy per vertex, $\epsilon_0(N.i)$ and $\epsilon_1(N.i)$, and the dimensionless magnetization squared per vertex,

Table 5. Comparison of our exact diagonalization estimates of ground state energy and magnetization with estimates by other methods.

Method of calculation	$\epsilon(\infty)$	$m_\perp(\infty)$
Exact diagonalization, all lattices	−1.0396	0.4803
Exact diagonalization, nonbipartite	−1.0389	0.4816
Spin wave, first order	−1.0380	0.4829
Spin wave, second order	−1.0406	0.4822
Series expansion, seven terms	−1.0408	0.4824

$m^2_{\perp,0}(N.i)$. For $N = 28$, 30 and 32 we used only the bipartite lattices because there are 99 nonbipartite even-N bcc lattices in this range. Similarly, on the odd-N bcc lattices of $9 \le N \le 31$ we computed $\epsilon_{1/2}(N.i)$, $\epsilon_{3/2}(N.i)$ and $m^2_{\perp,1/2}(N.i)$. Because it appeared of little physical significance we computed $m^2_{\perp,1}$ on only the bipartite lattices of $16 \le N \le 26$.

We used the same type of statistical analyses of the data described above as we had used in our previous paper [12]. The energy data statistically fitted to the appropriate three-term finite lattice scaling equation provided some interesting results. First Table 2 shows that within confidence limits $\epsilon_s(\infty)$ is independent of the spin S_z for at least $S_z = 0$, 1/2, 1 and 3/2. Furthermore, A^s_4, the coefficient of the second term in (7), $A^s_4 L^{-4}$, is also independent of S_z within confidence limits. However, A^s_6, the third term coefficient is decidedly dependent on S_z. Our findings for $\epsilon_s(\infty)$, A^s_4 and A^s_6 correspond to the general rules for finite size scaling equations as shown by Hasenfratz and Niedermayer [18]. The spin wave velocity, v, is determined by A_4, and the susceptibility, $\chi_\perp$, is determined by D_6. Hence the spin stiffness, ρ_s, is also estimated.

Turning to the magnetization per vertex, $m_{\perp,s}$, we calculated only the data for $m_{\perp,0}(N.i)$ and $m_{\perp,1/2}(N.i)$ for $N \le 32$. There are two reasons for not obtaining such data for $S_z(= s) > 1/2$. First, because it is obvious and well known that $m_{\perp,0}(\infty) = m_{\perp,s}(\infty)$. Second, because there is no known physical property analogous to the susceptibility obtained by studying $\epsilon_{s+1}(L) - \epsilon_s(L)$ as $L \to \infty$ as discussed on page 6.

At this point we compare our estimates of ϵ_0 and $m_\perp$ with spin wave and series expansion results of Oitmaa *et al.* [2] as displayed in Table 5. Unfortunately, they have not included additional terms in the scaling equations. Our average of exact diagonalization estimates of $\epsilon_s(\infty)$ is within 1% of the results of second order spin wave and a seven term series expansion. Our average estimate of $m_{\perp,s}(\infty)$ is within 2% of second order spin wave and series expansion results. All three methods could be used further to obtain more precise estimates of energy, magnetization, etc.

The finite three-dimensional lattices used so far are the three simplest: simple cubic, bcc and fcc lattices with complete cubic symmetry and only one vertex per unit cell. As computers advance various models on other lattices of lower symmetry and/or more vertices per unit cell could be studied. For example, perovskite lattices, for many manganites, have eight vertices per unit cell. The exact diagonalization method on finite lattices could eventually work on simple models of two states per vertex but at finite temperature. Much more can be just over the horizon.

We have received useful points from Prof. C.J. Hamer. This research has been supported in part by the Natural Sciences and Engineering Research Council of Canada, the Imperial Oil Charitable Foundation, and by Deutsche Forschungsgemeinschaft (project Ri 6151/1-2).

Appendix A: Geometric properties of finite bcc lattices

Each different bcc lattice is labelled $N.i$ where N is its number of vertices and i is the index distinguishing lattices of the same N.

Table A.1. Finite bcc lattices with an odd number of vertices, $9 \le N \le 31$.

$N.i$	$\mathbf{L}^{\mathrm{t}}_1$	$\mathbf{L}^{\mathrm{t}}_2$	$\mathbf{L}^{\mathrm{t}}_3$	I_{G}
9.13	(1, 1, 7)	(0, 2, 4)	(0, 0, 18)	0
11.15	(1, 1, 7)	(0, 2, 4)	(0, 0, 22)	0
13.17	(1, 1, 7)	(0, 2, 4)	(0, 0, 26)	2
13.18	(1, 1, 9)	(0, 2, 4)	(0, 0, 26)	0
15.19	(1, 1, 7)	(0, 2, 4)	(0, 0, 30)	4
15.20	(1, 1, 9)	(0, 2, 4)	(0, 0, 30)	2
15.21	(1, 1, 11)	(0, 2, 4)	(0, 0, 30)	2
15.28	(1, 1, 9)	(0, 2, 6)	(0, 0, 30)	2
15.30	(1, 1, 13)	(0, 2, 6)	(0, 0, 30)	2
15.38	(1, 1, 13)	(0, 2, 8)	(0, 0, 30)	2
15.577	(1, 3, 3)	(0, 6, 0)	(0, 0, 10)	0
17.22	(1, 1, 9)	(0, 2, 4)	(0, 0, 34)	2
17.23	(1, 1, 11)	(0, 2, 4)	(0, 0, 34)	0
17.24	(1, 1, 13)	(0, 2, 4)	(0, 0, 34)	2
17.25	(1, 1, 15)	(0, 2, 6)	(0, 0, 34)	2
19.24	(1, 1, 9)	(0, 2, 4)	(0, 0, 38)	2
19.25	(1, 1, 11)	(0, 2, 4)	(0, 0, 38)	0
19.26	(1, 1, 13)	(0, 2, 4)	(0, 0, 38)	0
19.27	(1, 1, 15)	(0, 2, 4)	(0, 0, 38)	4
19.37	(1, 1, 15)	(0, 2, 6)	(0, 0, 38)	2
19.38	(1, 1, 17)	(0, 2, 6)	(0, 0, 38)	4
21.26	(1, 1, 9)	(0, 2, 4)	(0, 0, 42)	4
21.27	(1, 1, 11)	(0, 2, 4)	(0, 0, 42)	0

Table A.1. Continued.

$N.i$	$\mathbf{L}_1^{\mathrm{t}}$	$\mathbf{L}_2^{\mathrm{t}}$	$\mathbf{L}_3^{\mathrm{t}}$	I_{G}
21.28	(1, 1, 13)	(0, 2, 4)	(0, 0, 42)	0
21.29	(1, 1, 15)	(0, 2, 4)	(0, 0, 42)	4
21.30	(1, 1, 17)	(0, 2, 4)	(0, 0, 42)	4
21.37	(1, 1, 9)	(0, 2, 6)	(0, 0, 42)	6
21.38	(1, 1, 11)	(0, 2, 6)	(0, 0, 42)	2
21.40	(1, 1, 15)	(0, 2, 6)	(0, 0, 42)	0
21.41	(1, 1, 17)	(0, 2, 6)	(0, 0, 42)	0
21.42	(1, 1, 19)	(0, 2, 6)	(0, 0, 42)	0
21.49	(1, 1, 11)	(0, 2, 8)	(0, 0, 42)	4
21.53	(1, 1, 19)	(0, 2, 8)	(0, 0, 42)	4
21.73	(1, 1, 15)	(0, 2, 12)	(0, 0, 42)	4
21.75	(1, 1, 19)	(0, 2, 12)	(0, 0, 42)	0
21.86	(1, 1, 19)	(0, 2, 14)	(0, 0, 42)	4
21.1332	(1, 3, 3)	(0, 6, 0)	(0, 0, 14)	0
23.28	(1, 1, 9)	(0, 2, 4)	(0, 0, 46)	6
23.29	(1, 1, 11)	(0, 2, 4)	(0, 0, 46)	0
23.30	(1, 1, 13)	(0, 2, 4)	(0, 0, 46)	2
23.31	(1, 1, 15)	(0, 2, 4)	(0, 0, 46)	2
23.32	(1, 1, 17)	(0, 2, 4)	(0, 0, 46)	8
23.33	(1, 1, 19)	(0, 2, 4)	(0, 0, 46)	2
23.41	(1, 1, 11)	(0, 2, 6)	(0, 0, 46)	4
23.45	(1, 1, 19)	(0, 2, 6)	(0, 0, 46)	6
23.46	(1, 1, 21)	(0, 2, 6)	(0, 0, 46)	2
23.53	(1, 1, 11)	(0, 2, 8)	(0, 0, 46)	6
23.56	(1, 1, 17)	(0, 2, 8)	(0, 0, 46)	6
25.30	(1, 1, 9)	(0, 2, 4)	(0, 0, 50)	8
25.31	(1, 1, 11)	(0, 2, 4)	(0, 0, 50)	2
25.32	(1, 1, 13)	(0, 2, 4)	(0, 0, 50)	2
25.33	(1, 1, 15)	(0, 2, 4)	(0, 0, 50)	4
25.34	(1, 1, 17)	(0, 2, 4)	(0, 0, 50)	4
25.36	(1, 1, 21)	(0, 2, 4)	(0, 0, 50)	2
25.44	(1, 1, 11)	(0, 2, 6)	(0, 0, 50)	6
25.45	(1, 1, 13)	(0, 2, 6)	(0, 0, 50)	6
25.49	(1, 1, 21)	(0, 2, 6)	(0, 0, 50)	8
25.50	(1, 1, 23)	(0, 2, 6)	(0, 0, 50)	4
25.58	(1, 1, 13)	(0, 2, 8)	(0, 0, 50)	2
25.59	(1, 1, 15)	(0, 2, 8)	(0, 0, 50)	8
25.72	(1, 1, 15)	(0, 2, 10)	(0, 0, 50)	2
25.4227	(1, 3, 5)	(0,10, 0)	(0, 0, 10)	2
27.33	(1, 1, 11)	(0, 2, 4)	(0, 0, 54)	4
27.34	(1, 1, 13)	(0, 2, 4)	(0, 0, 54)	2
27.35	(1, 1, 15)	(0, 2, 4)	(0, 0, 54)	6
27.36	(1, 1, 17)	(0, 2, 4)	(0, 0, 54)	4
27.39	(1, 1, 23)	(0, 2, 4)	(0, 0, 54)	2
27.49	(1, 1, 15)	(0, 2, 6)	(0, 0, 54)	4
27.51	(1, 1, 19)	(0, 2, 6)	(0, 0, 54)	2
27.52	(1, 1, 21)	(0, 2, 6)	(0, 0, 54)	4
27.53	(1, 1, 23)	(0, 2, 6)	(0, 0, 54)	4
27.54	(1, 1, 25)	(0, 2, 6)	(0, 0, 54)	4

Table A.1. Continued.

$N.i$	$\mathbf{L}_1^{\mathrm{t}}$	$\mathbf{L}_2^{\mathrm{t}}$	$\mathbf{L}_3^{\mathrm{t}}$	I_{G}
27.62	(1, 1, 13)	(0, 2, 8)	(0, 0, 54)	4
27.66	(1, 1, 21)	(0, 2, 8)	(0, 0, 54)	8
27.68	(1, 1, 25)	(0, 2, 8)	(0, 0, 54)	2
27.81	(1, 1, 23)	(0, 2, 10)	(0, 0, 54)	4
27.91	(1, 1, 15)	(0, 2, 12)	(0, 0, 54)	8
27.94	(1, 1, 21)	(0, 2, 12)	(0, 0, 54)	6
27.124	(1, 1, 25)	(0, 2, 16)	(0, 0, 54)	4
27.136	(1, 1, 21)	(0, 2, 18)	(0, 0, 54)	8
27.2354	(1, 1, 5)	(0, 6, 0)	(0, 0, 18)	2
27.2396	(1, 1, 5)	(0, 6, 6)	(0, 0, 18)	0
27.2399	(1, 1, 11)	(0, 6, 6)	(0, 0, 18)	4
27.2549	(1, 3, 3)	(0, 6, 0)	(0, 0, 18)	4
27.2550	(1, 3, 5)	(0, 6, 0)	(0, 0, 18)	2
27.2594	(1, 3, 9)	(0, 6, 6)	(0, 0, 18)	2
27.14309	(3, 3, 3)	(0, 6, 0)	(0, 0, 6)	0
29.35	(1, 1, 11)	(0, 2, 4)	(0, 0, 58)	4
29.36	(1, 1, 13)	(0, 2, 4)	(0, 0, 58)	2
29.37	(1, 1, 15)	(0, 2, 4)	(0, 0, 58)	4
29.38	(1, 1, 17)	(0, 2, 4)	(0, 0, 58)	6
29.39	(1, 1, 19)	(0, 2, 4)	(0, 0, 58)	4
29.41	(1, 1, 23)	(0, 2, 4)	(0, 0, 58)	8
29.42	(1, 1, 25)	(0, 2, 4)	(0, 0, 58)	2
29.50	(1, 1, 11)	(0, 2, 6)	(0, 0, 58)	10
29.51	(1, 1, 13)	(0, 2, 6)	(0, 0, 58)	8
29.52	(1, 1, 15)	(0, 2, 6)	(0, 0, 58)	2
29.55	(1, 1, 21)	(0, 2, 6)	(0, 0, 58)	8
29.57	(1, 1, 25)	(0, 2, 6)	(0, 0, 58)	4
29.58	(1, 1, 27)	(0, 2, 6)	(0, 0, 58)	4
29.66	(1, 1, 13)	(0, 2, 8)	(0, 0, 58)	4
29.73	(1, 1, 27)	(0, 2, 8)	(0, 0, 58)	4
29.85	(1, 1, 21)	(0, 2, 10)	(0, 0, 58)	8
31.37	(1, 1, 11)	(0, 2, 4)	(0, 0, 62)	4
31.38	(1, 1, 13)	(0, 2, 4)	(0, 0, 62)	2
31.39	(1, 1, 15)	(0, 2, 4)	(0, 0, 62)	2
31.40	(1, 1, 17)	(0, 2, 4)	(0, 0, 62)	8
31.41	(1, 1, 19)	(0, 2, 4)	(0, 0, 62)	4
31.44	(1, 1, 25)	(0, 2, 4)	(0, 0, 62)	4
31.45	(1, 1, 27)	(0, 2, 4)	(0, 0, 62)	2
31.54	(1, 1, 13)	(0, 2, 6)	(0, 0, 62)	10
31.55	(1, 1, 15)	(0, 2, 6)	(0, 0, 62)	2
31.58	(1, 1, 21)	(0, 2, 6)	(0, 0, 62)	2
31.59	(1, 1, 23)	(0, 2, 6)	(0, 0, 62)	8
31.61	(1, 1, 27)	(0, 2, 6)	(0, 0, 62)	6
31.62	(1, 1, 29)	(0, 2, 6)	(0, 0, 62)	4
31.71	(1, 1, 15)	(0, 2, 8)	(0, 0, 62)	8
31.74	(1, 1, 21)	(0, 2, 8)	(0, 0, 62)	4
31.78	(1, 1, 29)	(0, 2, 8)	(0, 0, 62)	4
31.94	(1, 1, 29)	(0, 2, 10)	(0, 0, 62)	2

Table A.2. Finite bcc lattices with an even number of lattices, $10 \leq N \leq 26$.

$N.i$	$\mathbf{L}_1^{\mathrm{t}}$	$\mathbf{L}_2^{\mathrm{t}}$	$\mathbf{L}_3^{\mathrm{t}}$	I_{G}
10.15	(1, 1, 7)	(0, 2, 4)	(0, 0, 20)	0
12.25	(1, 1, 9)	(0, 2, 6)	(0, 0, 24)	0
12.17	(1, 1, 7)	(0, 2, 4)	(0, 0, 24)	1
14.21	(1, 1, 11)	(0, 2, 4)	(0, 0, 28)	1
14.20	(1, 1, 9)	(0, 2, 4)	(0, 0, 28)	2
14.19	(1, 1, 7)	(0, 2, 4)	(0, 0, 28)	3
16.23	(1, 1, 11)	(0, 2, 4)	(0, 0, 32)	0
16.1642	(2, 0, 8)	(0, 2, 4)	(0, 0, 16)	1
16.41	(1, 1, 11)	(0, 2, 8)	(0, 0, 32)	2
16.24	(1, 1, 13)	(0, 2, 4)	(0, 0, 32)	3
16.32	(1, 1, 11)	(0, 2, 6)	(0, 0, 32)	3
16.21	(1, 1, 7)	(0, 2, 4)	(0, 0, 32)	5
18.37	(1, 1, 15)	(0, 2, 6)	(0, 0, 36)	0
18.25	(1, 1, 11)	(0, 2, 4)	(0, 0, 36)	1
18.1101	(1, 3, 3)	(0, 6, 0)	(0, 0, 12)	1
18.2024	(2, 0, 8)	(0, 2, 4)	(0, 0, 18)	1
18.24	(1, 1, 9)	(0, 2, 4)	(0, 0, 36)	2
18.26	(1, 1, 13)	(0, 2, 4)	(0, 0, 36)	2
18.35	(1, 1, 11)	(0, 2, 6)	(0, 0, 36)	2
18.36	(1, 1, 13)	(0, 2, 6)	(0, 0, 36)	2
18.1001	(1, 1, 3)	(0, 6, 0)	(0, 0, 12)	2
18.27	(1, 1, 15)	(0, 2, 4)	(0, 0, 36)	3
18.34	(1, 1, 9)	(0, 2, 6)	(0, 0, 36)	4
18.67	(1, 1, 15)	(0, 2, 12)	(0, 0, 36)	5
20.27	(1, 1, 11)	(0, 2, 4)	(0, 0, 40)	0
20.50	(1, 1, 13)	(0, 2, 8)	(0, 0, 40)	0
20.30	(1, 1, 17)	(0, 2, 4)	(0, 0, 40)	1
20.62	(1, 1, 15)	(0, 2, 10)	(0, 0, 40)	1
20.630	(1, 1, 7)	(0, 4, 4)	(0, 0, 20)	2
20.2446	(2, 0, 8)	(0, 2, 4)	(0, 0, 20)	2
20.26	(1, 1, 9)	(0, 2, 4)	(0, 0, 40)	3
20.38	(1, 1, 11)	(0, 2, 6)	(0, 0, 40)	3
20.61	(1, 1, 13)	(0, 2, 10)	(0, 0, 40)	3
20.2447	(2, 0,10)	(0, 2, 4)	(0, 0, 20)	3
20.73	(1, 1, 15)	(0, 2, 12)	(0, 0, 40)	4
20.629	(1, 1, 5)	(0, 4, 4)	(0, 0, 20)	4
20.29	(1, 1, 15)	(0, 2, 4)	(0, 0, 40)	5
20.40	(1, 1, 15)	(0, 2, 6)	(0, 0, 40)	5
20.63	(1, 1, 17)	(0, 2,10)	(0, 0, 40)	5
20.51	(1, 1, 15)	(0, 2, 8)	(0, 0, 40)	6
22.29	(1, 1, 11)	(0, 2, 4)	(0, 0, 44)	0
22.33	(1, 1, 19)	(0, 2, 4)	(0, 0, 44)	1
22.31	(1, 1, 15)	(0, 2, 4)	(0, 0, 44)	2
22.43	(1, 1, 15)	(0, 2, 6)	(0, 0, 44)	2
22.44	(1, 1, 17)	(0, 2, 6)	(0, 0, 44)	4
22.30	(1, 1, 13)	(0, 2, 4)	(0, 0, 44)	3

Table A.2. Continued.

$N.i$	$\mathbf{L}_1^{\mathrm{t}}$	$\mathbf{L}_2^{\mathrm{t}}$	$\mathbf{L}_3^{\mathrm{t}}$	I_{G}
22.2908	(2, 0, 8)	(0, 2, 4)	(0, 0, 22)	3
22.41	(1, 1, 11)	(0, 2, 6)	(0, 0, 44)	4
22.28	(1, 1, 9)	(0, 2, 4)	(0, 0, 44)	5
22.66	(1, 1, 13)	(0, 2, 10)	(0, 0, 44)	5
22.69	(1, 1, 19)	(0, 2, 10)	(0, 0, 44)	5
22.42	(1, 1, 13)	(0, 2, 6)	(0, 0, 44)	6
22.32	(1, 1, 17)	(0, 2, 4)	(0, 0, 44)	7
24.30	(1, 1, 9)	(0, 2, 4)	(0, 0, 48)	7
24.31	(1, 1, 11)	(0, 2, 4)	(0, 0, 48)	1
24.32	(1, 1, 13)	(0, 2, 4)	(0, 0, 48)	2
24.33	(1, 1, 15)	(0, 2, 4)	(0, 0, 48)	2
24.34	(1, 1, 17)	(0, 2, 4)	(0, 0, 48)	8
24.36	(1, 1, 21)	(0, 2, 4)	(0, 0, 48)	1
24.44	(1, 1, 11)	(0, 2, 6)	(0, 0, 48)	6
24.45	(1, 1, 13)	(0, 2, 6)	(0, 0, 48)	8
24.46	(1, 1, 15)	(0, 2, 6)	(0, 0, 48)	5
24.47	(1, 1, 17)	(0, 2, 6)	(0, 0, 48)	1
24.48	(1, 1, 19)	(0, 2, 6)	(0, 0, 48)	1
24.49	(1, 1, 21)	(0, 2, 6)	(0, 0, 48)	1
24.57	(1, 1, 11)	(0, 2, 8)	(0, 0, 48)	7
24.58	(1, 1, 13)	(0, 2, 8)	(0, 0, 48)	1
24.59	(1, 1, 15)	(0, 2, 8)	(0, 0, 48)	6
24.61	(1, 1, 19)	(0, 2, 8)	(0, 0, 48)	8
24.71	(1, 1, 13)	(0, 2, 10)	(0, 0, 48)	5
24.73	(1, 1, 17)	(0, 2, 10)	(0, 0, 48)	5
24.86	(1, 1, 17)	(0, 2, 12)	(0, 0, 48)	2
24.87	(1, 1, 19)	(0, 2, 12)	(0, 0, 48)	4
24.88	(1, 1, 21)	(0, 2, 12)	(0, 0, 48)	3
24.100	(1, 1, 19)	(0, 2, 14)	(0, 0, 48)	3
24.113	(1, 1, 19)	(0, 2, 16)	(0, 0, 48)	6
24.873	(1, 1, 5)	(0, 4, 4)	(0, 0, 24)	6
24.875	(1, 1, 9)	(0, 4, 4)	(0, 0, 24)	6
24.888	(1, 1, 9)	(0, 4, 6)	(0, 0, 24)	2
24.894	(1, 1, 21)	(0, 4, 6)	(0, 0, 24)	6
24.1860	(1, 3, 3)	(0, 6, 0)	(0, 0, 16)	2
24.1911	(1, 3, 1)	(0, 6, 8)	(0, 0, 16)	6
24.2705	(1, 3, 3)	(0, 8, 0)	(0, 0, 12)	3
24.3410	(2, 0, 8)	(0, 2, 4)	(0, 0, 24)	4
24.3411	(2, 0, 10)	(0, 2, 4)	(0, 0, 24)	4
24.3424	(2, 0, 10)	(0, 2, 6)	(0, 0, 24)	4
24.4266	(2, 0, 4)	(0, 4, 6)	(0, 0, 12)	4
24.3412	(2, 0, 12)	(0, 2, 4)	(0, 0, 24)	5
24.3425	(2, 0, 12)	(0, 2, 6)	(0, 0, 24)	5
26.33	(1, 1, 11)	(0, 2, 4)	(0, 0, 52)	3
26.34	(1, 1, 13)	(0, 2, 4)	(0, 0, 52)	2
26.35	(1, 1, 15)	(0, 2, 4)	(0, 0, 52)	7
26.36	(1, 1, 17)	(0, 2, 4)	(0, 0, 52)	4

Table A.2. Continued.

$N.i$	$\mathbf{L}_1^{\mathrm{t}}$	$\mathbf{L}_2^{\mathrm{t}}$	$\mathbf{L}_3^{\mathrm{t}}$	I_{G}
26.38	(1, 1, 21)	(0, 2, 4)	(0, 0, 52)	5
26.39	(1, 1, 23)	(0, 2, 4)	(0, 0, 52)	3
26.47	(1, 1, 11)	(0, 2, 6)	(0, 0, 52)	7
26.48	(1, 1, 13)	(0, 2, 6)	(0, 0, 52)	8
26.49	(1, 1, 15)	(0, 2, 6)	(0, 0, 52)	4
26.50	(1, 1, 17)	(0, 2, 6)	(0, 0, 52)	4
26.51	(1, 1, 19)	(0, 2, 6)	(0, 0, 52)	8
26.52	(1, 1, 21)	(0, 2, 6)	(0, 0, 52)	7
26.61	(1, 1, 11)	(0, 2, 8)	(0, 0, 52)	9
26.76	(1, 1, 13)	(0, 2, 10)	(0, 0, 52)	8
26.78	(1, 1, 17)	(0, 2, 10)	(0, 0, 52)	4
26.92	(1, 1, 17)	(0, 2, 12)	(0, 0, 52)	3
26.122	(1, 1, 21)	(0, 2, 16)	(0, 0, 52)	5
26.5912	(2, 0, 8)	(0, 2, 4)	(0, 0, 26)	5
26.5913	(2, 0, 10)	(0, 2, 4)	(0, 0, 26)	5

Table A.3. Bipartite finite lattices with $28 \leq N \leq 32$.

$N.i$	$\mathbf{L}_1^{\mathrm{t}}$	$\mathbf{L}_2^{\mathrm{t}}$	$\mathbf{L}_3^{\mathrm{t}}$	I_{G}
28.6785	(2, 0, 10)	(0, 2, 4)	(0, 0, 28)	5
28.6786	(2, 0, 12)	(0, 2, 4)	(0, 0, 28)	5
28.6816	(2, 0, 12)	(0, 2, 8)	(0, 0, 28)	5
28.6784	(2, 0, 8)	(0, 2, 4)	(0, 0, 28)	7
28.6800	(2, 0, 10)	(0, 2, 6)	(0, 0, 28)	7
30.7717	(2, 0, 10)	(0, 2, 4)	(0, 0, 30)	4
30.7718	(2, 0, 12)	(0, 2, 4)	(0, 0, 30)	4
30.7733	(2, 0, 10)	(0, 2, 6)	(0, 0, 30)	4
30.7734	(2, 0, 12)	(0, 2, 6)	(0, 0, 30)	4
30.7750	(2, 0, 12)	(0, 2, 8)	(0, 0, 30)	4
30.7716	(2, 0, 8)	(0, 2, 4)	(0, 0, 30)	8
30.10754	(2, 0, 4)	(0, 6, 0)	(0, 0, 10)	7
32.8710	(2, 0, 12)	(0, 2, 4)	(0, 0, 32)	3
32.8709	(2, 0, 10)	(0, 2, 4)	(0, 0, 32)	5
32.8726	(2, 0, 10)	(0, 2, 6)	(0, 0, 32)	7
32.8745	(2, 0, 14)	(0, 2, 8)	(0, 0, 32)	7
32.10441	(2, 0, 6)	(0, 4, 4)	(0, 0, 16)	7
32.10475	(2, 0, 6)	(0, 4, 8)	(0, 0, 16)	7
32.8729	(2, 0, 16)	(0, 2, 6)	(0, 0, 32)	8
32.8744	(2, 0, 12)	(0, 2, 8)	(0, 0, 32)	6
32.10474	(2, 0, 4)	(0, 4, 8)	(0, 0, 16)	6
32.10440	(2, 0, 4)	(0, 4, 4)	(0, 0, 16)	8
32.8708	(2, 0, 8)	(0, 2, 4)	(0, 0, 32)	10
32.14163	(2, 2, 4)	(0, 8, 0)	(0, 0, 8)	10
32.27780	(4, 0, 4)	(0, 4, 4)	(0, 0, 8)	10
32.14452	(2, 4, 4)	(0, 8, 0)	(0, 0, 8)	10
32.8711	(2, 0, 14)	(0, 2, 4)	(0, 0, 32)	10

Appendix B: Dimensionless lowest energies, ϵ_{s}, per vertex and magnetization squared, $\mathsf{m}^2_{\mathsf{x,s}}$, per vertex on finite lattice bcc lattices

Table B.1. Lowest energies per vertex, $\epsilon_{1/2}$ and $\epsilon_{3/2}$ for $S = 1/2$ and $S = 3/2$ and highest magnetizations squared for $S = 1/2$ on odd-N bcc lattices.

$N.i$	$\epsilon_{1/2}$	$\epsilon_{3/2}$	$m^2_{x,1/2}$
9.13	−1.111111	−1.000000	0.151235
11.15	−1.097845	−1.024081	0.145971
13.17	−1.089331	−1.036804	0.142017
13.18	−1.087852	−1.035348	0.142359
15.19	−1.084328	−1.045012	0.138698
15.20	−1.080184	−1.040916	0.139706
15.21	−1.081390	−1.042115	0.139452
15.28	−1.081370	−1.042097	0.139461
15.30	−1.082254	−1.042970	0.139267
15.38	−1.080958	−1.041686	0.139545
15.577	−1.080803	−1.041537	0.139598
17.22	−1.075262	−1.044788	0.137883
17.23	−1.074157	−1.043685	0.138107
17.24	−1.076656	−1.046173	0.137558
17.25	−1.076804	−1.046316	0.137506
19.24	−1.071814	−1.047477	0.135870
19.25	−1.069375	−1.045045	0.136405
19.26	−1.070551	−1.046218	0.136149
19.27	−1.073684	−1.049329	0.135368
19.37	−1.073588	−1.049235	0.135392
19.38	−1.071901	−1.047561	0.135846
21.26	−1.069336	−1.049447	0.134105
21.27	−1.066292	−1.046420	0.134862
21.28	−1.065706	−1.045831	0.134968
21.29	−1.070156	−1.050258	0.133858
21.30	−1.070145	−1.050248	0.133862
21.31	−1.071393	−1.051487	0.133500
21.38	−1.068786	−1.048905	0.134315
21.40	−1.068096	−1.048216	0.134435
21.41	−1.067288	−1.047416	0.134672
21.42	−1.066522	−1.046651	0.134830
21.49	−1.069085	−1.049199	0.134209
21.53	−1.071373	−1.051466	0.133509
21.73	−1.070043	−1.050148	0.133892
21.75	−1.066387	−1.046512	0.134834
21.86	−1.069112	−1.049225	0.134195
21.1332	−1.067424	−1.047550	0.134627
23.28	−1.067501	−1.050940	0.132537
23.29	−1.063762	−1.047226	0.133571
23.30	−1.063050	−1.046508	0.133671
23.31	−1.064184	−1.047640	0.133436

Table B.1. Continued.

$N.i$	$\epsilon_{1/2}$	$\epsilon_{3/2}$	$m^2_{x,1/2}$
23.32	−1.069743	−1.053165	0.131821
23.33	−1.065691	−1.049142	0.133032
23.41	−1.066641	−1.050091	0.132890
23.45	−1.067099	−1.050543	0.132701
23.46	−1.063846	−1.047307	0.133546
23.53	−1.067190	−1.050632	0.132680
23.56	−1.069550	−1.052975	0.131895
25.30	−1.066090	−1.052086	0.131130
25.31	−1.061896	−1.047917	0.132392
25.32	−1.060664	−1.046687	0.132673
25.33	−1.061319	−1.047334	0.132442
25.34	−1.064092	−1.050099	0.131729
25.36	−1.062042	−1.048061	0.132336
25.44	−1.064898	−1.050907	0.131648
25.45	−1.064961	−1.050967	0.131639
25.49	−1.065471	−1.051473	0.131416
25.50	−1.062058	−1.048076	0.132346
25.58	−1.061775	−1.047798	0.132432
25.59	−1.065589	−1.051589	0.131353
25.72	−1.060732	−1.046755	0.132656
25.4227	−1.060729	−1.046751	0.132658
27.33	−1.060436	−1.048462	0.131329
27.34	−1.058698	−1.046732	0.131791
27.35	−1.059906	−1.047926	0.131353
27.36	−1.059721	−1.047747	0.131497
27.39	−1.059268	−1.047300	0.131647
27.49	−1.060493	−1.048519	0.131297
27.51	−1.060438	−1.048467	0.131391
27.52	−1.061408	−1.049434	0.131151
27.53	−1.060734	−1.048761	0.131285
27.54	−1.059340	−1.047370	0.131628
27.62	−1.060233	−1.048262	0.131408
27.66	−1.063687	−1.051699	0.130483
27.68	−1.059064	−1.047098	0.131711
27.81	−1.060187	−1.048216	0.131432
27.91	−1.063222	−1.051240	0.130677
27.94	−1.062741	−1.050755	0.130577
27.124	−1.059294	−1.047321	0.131584
27.136	−1.063248	−1.051266	0.130664
27.2354	−1.059580	−1.047612	0.131592
27.2396	−1.058818	−1.046855	0.131794
27.2399	−1.059844	−1.047868	0.131453
27.2549	−1.061395	−1.049421	0.131156
27.2550	−1.059735	−1.047765	0.131538
27.2594	−1.060740	−1.048769	0.131342
27.14309	−1.060109	−1.048142	0.131513
29.35	−1.059263	−1.048892	0.130361

Table B.1. Continued.

$N.i$	$\epsilon_{1/2}$	$\epsilon_{3/2}$	$m^2_{x,1/2}$
29.36	−1.057294	−1.046932	0.130926
29.37	−1.057856	−1.047488	0.130734
29.38	−1.058752	−1.048376	0.130369
29.39	−1.059394	−1.049022	0.130310
29.41	−1.061719	−1.051336	0.129510
29.42	−1.057354	−1.046991	0.130912
29.50	−1.062484	−1.052101	0.129494
29.51	−1.062027	−1.051648	0.129725
29.52	−1.058575	−1.048210	0.130630
29.55	−1.062289	−1.051908	0.129609
29.57	−1.058853	−1.048486	0.130533
29.58	−1.057423	−1.047059	0.130894
29.66	−1.058950	−1.048582	0.130483
29.73	−1.059037	−1.048667	0.130458
29.85	−1.062309	−1.051928	0.129597
31.37	−1.058318	−1.049248	0.129470
31.38	−1.056109	−1.047048	0.130164
31.39	−1.056223	−1.047161	0.130125
31.40	−1.057808	−1.048734	0.129468
31.41	−1.056782	−1.047715	0.129914
31.44	−1.058351	−1.049280	0.129450
31.45	−1.056228	−1.047166	0.130120
31.54	−1.060975	−1.051898	0.128894
31.55	−1.057395	−1.048331	0.129846
31.58	−1.057387	−1.048323	0.129871
31.59	−1.061060	−1.051982	0.128849
31.61	−1.057905	−1.048838	0.129643
31.62	−1.056273	−1.047210	0.130115
31.71	−1.061290	−1.052210	0.128746
31.74	−1.057821	−1.048754	0.129694
31.78	−1.057971	−1.048902	0.129631
31.94	−1.055874	−1.046815	0.130243

Table B.2. Lowest energies per vertex, ϵ_0 and ϵ_1 for $S = 0$ and $S = 1$ and highest magnetizations squared for $S = 0$ on even-N bcc lattices.

$N.i$	ϵ_0	ϵ_1	$m^2_{x,0}$
10.15	−1.115022	−1.070219	0.149610
12.25	−1.099498	−1.068599	0.145017
12.17	−1.100778	−1.069868	0.144744
14.21	−1.090423	−1.067827	0.141360
14.20	−1.089310	−1.066715	0.141581
14.19	−1.092238	−1.069629	0.140898
16.23	−1.081668	−1.064433	0.139034
16.1642	−1.078975	−1.061714	0.139531
16.41	−1.083024	−1.065785	0.138724

Table B.2. Continued.

$N.i$	ϵ_0	ϵ_1	$m^2_{x,0}$
16.24	−1.082957	−1.065720	0.138750
16.32	−1.083102	−1.065864	0.138698
16.21	−1.086794	−1.069535	0.137714
18.37	−1.076639	−1.063062	0.136877
18.25	−1.074930	−1.061351	0.137208
18.1101	−1.076270	−1.062694	0.136951
18.2024	−1.073869	−1.060277	0.137399
18.24	−1.076782	−1.063203	0.136829
18.26	−1.077395	−1.063814	0.136668
18.35	−1.077087	−1.063509	0.136777
18.36	−1.078914	−1.065327	0.136301
18.1001	−1.077833	−1.064251	0.136573
18.27	−1.077572	−1.063989	0.136612
18.34	−1.078467	−1.064883	0.136401
18.67	−1.078797	−1.065210	0.136273
20.27	−1.070541	−1.059569	0.135571
20.50	−1.071442	−1.060473	0.135405
20.30	−1.071890	−1.060915	0.135254
20.62	−1.069670	−1.058694	0.135723
20.630	−1.072857	−1.061883	0.135087
20.2446	−1.069862	−1.058882	0.135678
20.26	−1.073220	−1.062244	0.134948
20.38	−1.073013	−1.062039	0.135028
20.61	−1.075150	−1.064166	0.134404
20.2447	−1.069906	−1.058925	0.135662
20.73	−1.073071	−1.062096	0.135005
20.629	−1.072875	−1.061902	0.135078
20.29	−1.075189	−1.064205	0.134393
20.40	−1.075014	−1.064032	0.134456
20.63	−1.075106	−1.064122	0.134428
20.51	−1.075166	−1.064181	0.134409
22.29	−1.067179	−1.058131	0.134195
22.33	−1.067353	−1.058303	0.134137
22.31	−1.069031	−1.059977	0.133699
22.43	−1.068563	−1.059512	0.133873
22.30	−1.066438	−1.057386	0.134304
22.2908	−1.066695	−1.057639	0.134236
22.41	−1.069958	−1.060905	0.133547
22.28	−1.070624	−1.061566	0.133285
22.66	−1.070377	−1.061321	0.133389
22.69	−1.072611	−1.063546	0.132684
22.42	−1.070401	−1.061344	0.133389
22.32	−1.072775	−1.063709	0.132625
22.44	−1.069958	−1.060905	0.133547
24.30	−1.068651	−1.061048	0.131805
24.31	−1.064665	−1.057074	0.132955
24.32	−1.063751	−1.056158	0.133125
24.33	−1.064305	−1.056710	0.132992

Table B.2. Continued.

$N.i$	ϵ_0	ϵ_1	$m^2_{x,0}$
24.34	−1.069432	−1.061826	0.131549
24.36	−1.063865	−1.056275	0.133138
24.44	−1.067580	−1.059983	0.132255
24.45	−1.068202	−1.060602	0.131999
24.46	−1.065818	−1.058222	0.132573
24.47	−1.064946	−1.057355	0.132915
24.48	−1.065731	−1.058140	0.132746
24.49	−1.065218	−1.057626	0.132816
24.57	−1.068174	−1.060573	0.132021
24.58	−1.064527	−1.056937	0.133002
24.59	−1.068478	−1.060878	0.131977
24.61	−1.070772	−1.063162	0.131121
24.71	−1.067526	−1.059929	0.132284
24.73	−1.065990	−1.058392	0.132524
24.86	−1.063825	−1.056235	0.133149
24.87	−1.064988	−1.057394	0.132854
24.88	−1.066667	−1.059070	0.132372
24.100	−1.063459	−1.055869	0.133222
24.113	−1.067629	−1.060032	0.132236
24.873	−1.067678	−1.060081	0.132218
24.875	−1.068331	−1.060732	0.132032
24.888	−1.066408	−1.058814	0.132557
24.894	−1.067585	−1.059988	0.132259
24.1860	−1.065748	−1.058156	0.132743
24.1911	−1.068268	−1.060669	0.132057
24.2705	−1.066061	−1.058468	0.132619
24.3410	−1.064190	−1.056594	0.132986
24.3411	−1.064043	−1.056447	0.133043
24.3424	−1.063994	−1.056399	0.133061
24.4266	−1.063990	−1.056395	0.133064
24.3412	−1.064285	−1.056688	0.132950
24.3425	−1.064697	−1.057097	0.132787
26.33	−1.062746	−1.056285	0.131835
26.34	−1.061196	−1.054738	0.132228
26.35	−1.062356	−1.055891	0.131810
26.36	−1.063033	−1.056570	0.131737
26.38	−1.064957	−1.058490	0.131140
26.39	−1.061341	−1.054882	0.132183
26.47	−1.065798	−1.059332	0.131066
26.48	−1.065874	−1.059407	0.131037
26.49	−1.062641	−1.056180	0.131875
26.50	−1.062636	−1.056176	0.131878
26.51	−1.065896	−1.059429	0.131026
26.52	−1.065720	−1.059254	0.131108
26.61	−1.066418	−1.059948	0.130806
26.76	−1.065989	−1.059521	0.131004
26.78	−1.064163	−1.057699	0.131481
26.92	−1.063033	−1.056570	0.131737

Table B.2. Continued.

$N.i$	ϵ_0	ϵ_1	$m^2_{x,0}$
26.122	−1.061352	−1.054894	0.132167
26.5912	−1.062218	−1.055753	0.131869
26.5913	−1.061799	−1.055336	0.132039
28.6785	−1.059855	−1.054290	0.131187
28.6786	−1.060332	−1.054765	0.130993
28.6816	−1.060055	−1.054489	0.131109
28.6784	−1.060669	−1.055100	0.130850
28.6800	−1.059807	−1.054242	0.131206
30.7717	−1.058308	−1.053465	0.130397
30.7718	−1.058525	−1.053681	0.130307
30.7733	−1.058113	−1.053270	0.130473
30.7734	−1.058524	−1.053680	0.130309
30.7750	−1.058751	−1.053906	0.130211
30.7716	−1.059447	−1.054599	0.129908
30.10754	−1.058525	−1.053681	0.130309
32.8710	−1.056918	−1.052665	0.129722
32.8709	−1.057082	−1.052828	0.129654
32.8726	−1.056915	−1.052663	0.129500
32.8745	−1.057128	−1.052874	0.129604
32.10441	−1.056711	−1.052459	0.129724
32.10475	−1.057036	−1.052783	0.129636
32.8729	−1.057217	−1.052963	0.129805
32.8744	−1.057455	−1.053200	0.129670
32.10474	−1.057218	−1.052964	0.129604
32.10440	−1.057957	−1.053701	0.129270
32.8708	−1.058465	−1.054207	0.129035
32.14163	−1.057220	−1.052966	0.129602
32.27780	−1.056805	−1.052552	0.129438
32.14452	−1.057632	−1.053376	0.129770
32.8711	−1.057914	−1.053658	0.128926

References

1. R.R.P. Singh, Phys. Rev. B **39**, 9760 (1989).
2. J. Oitmaa, C.J. Hamer, Zheng Weihong, Phys. Rev. B **50**, 3877 (1994).
3. P.W. Anderson, Phys. Rev. **86**, 694 (1952).
4. R. Kubo, Phys. Rev. **87**, 568 (1952).
5. G. Gomez-Santos, J.D. Joannopoulos, Phys. Rev. B **36**, 8707 (1987).
6. M. Suzuki, S. Miyashita, Can. J. Phys. **56**, 902 (1978).
7. C.J. Hamer, T. Hövelborn, M. Bachhuber, J. Phys. A **32**, 51 (1999).
8. A.W. Sandvik, C.J. Hamer, Phys. Rev. B **60**, 6588 (1999).
9. D.D. Betts, H.-Q. Lin, J.S. Flynn, Can. J. Phys. **77**, 353 (1999).
10. D.D. Betts, G. Stewart, Can. J. Phys. **75**, 47 (1997).
11. G.E. Stewart, D.D. Betts, J.S. Flynn, J. Phys. Soc. Jpn **66**, 3231 (1997).
12. D.D. Betts, J. Schulenburg, G.E. Stewart, J. Richter, J.S. Flynn, J. Phys. A **31**, 7685 (1998).
13. J.N. Lyness, T. Sorevik, P. Keast, Math. Comp. **56**, 243 (1991).
14. E.H. Lieb, D.C. Mattis, J. Math. Phys. **3**, 749 (1962).
15. T. Kennedy, E.H. Lieb, B.S. Shastry, J. Stat. Phys. **53**, 1019 (1988).
16. K. Kubo, T. Kishi, Phys. Rev. Lett. **61**, 2585 (1988).
17. J.K. Cullum, R.A. Willoughby, *Introduction to the Theory of Canonical Matrices* (Blackie, 1932).
18. P. Hasenfratz, F. Niedermayer, Z. Phys. B **92**, 91 (1993).
19. P. Hasenfratz, H. Leutwyler, Nucl. Phys. **343**, 241 (1990).
20. H. Neuberger, T.A.L. Ziman, Phys. Rev. B **39**, 2608 (1989).
21. D.S. Fisher, Phys. Rev. B **39**, 11783 (1989).